Nanoscale

RSC Publishing

PAPER

View Article Online
View Journal | View Issue

Cite this: *Nanoscale*, 2013, **5**, 4436

Effect of the surface-plasmon–exciton coupling and charge transfer process on the photoluminescence of metal–semiconductor nanostructures†

Jun Yin,[a] Chuang Yue,[b] Yashu Zang,[b] Ching-Hsueh Chiu,[c] Jinchai Li,[b] Hao-Chung Kuo,[c] Zhihao Wu,*[a] Jing Li,*[b] Yanyan Fang[a] and Changqing Chen[a]

Received 21st February 2013
Accepted 19th March 2013

DOI: 10.1039/c3nr00920c

www.rsc.org/nanoscale

The effect of direct metal coating on the photoluminescence (PL) properties of ZnO nanorods (NRs) has been investigated in detail in this work. The direct coating of Ag nanoparticles (NPs) induces remarkable enhancement of the surface exciton (SX) emissions from the ZnO NRs. Meanwhile, the charge transfer process between ZnO and Ag also leads to notable increment of blue and violet emissions from Zn interstitial defects. A thin SiO_2 blocking layer inserted between the ZnO and Ag has been demonstrated to be able to efficiently suppress the defect emission enhancement caused by the direct contact of metal–semiconductor, without weakening the surface-plasmon–exciton coupling effect. A theoretical model considering the type of contacts formed between metals, ZnO and blocking layer is proposed to interpret the change of the PL spectra.

Introduction

The surface plasmon (SP)–exciton coupling effect shows attractive properties in enhancing spontaneous recombination rate and emission efficiency in semiconductor materials or luminescent materials[1] and has the potential applications in optoelectronic devices, such as light-emitting diodes (LEDs).[2–5] Most of the current work focuses on the enhancement of band edge emission and the suppression of defect emission by introducing the metal nanostructures. However, the influence of surface state changes due to the metal nanostructure coating on the photoluminescence properties of semiconductors is not yet clear, especially for nanostructured materials, such as nanorods (NRs) or nanowires (NWs), which are particularly susceptible to the surface conditions due to the large surface-to-volume ratio determined by the small sizes of nanostructures.

ZnO, with its wide direct band gap ($E_g = 3.37$ eV at 300 K) and large free-exciton binding energy (60 meV), is an attractive semiconductor for optoelectronic applications in the ultraviolet spectrum and for transparent electronic devices. In particular, ZnO NWs and NRs have attracted renewed attention in recent years due to their peculiar optical properties.[6–9] Due to the large surface-to-volume ratio determined by the small diameters of NRs, these structures are ideal for investigating the influence of surface effects on their optical properties. Early reports have demonstrated that the photoluminescence (PL) properties of ZnO NRs or NWs would be deeply influenced by coating external dielectric materials, such as polymers and Al_2O_3, which can modify the surface states of ZnO nanostructures.[10–12]

In this work, the influences of coated Ag nanoparticles (NPs) on the PL properties of ZnO NRs have been systematically studied by temperature dependent PL (TDPL) and time-resolved PL (TRPL). Low temperature PL spectra of the as-grown ZnO NRs are dominated by near band edge (NBE) emission originated from the defect bound excitons (DBXs) and their phonon replicas. After the direct coating of Ag NPs on the surface of ZnO NRs, the surface exciton (SX) emission, as well as the defect emission of ZnO NRs, is remarkably enhanced. After introducing a 10 nm SiO_2 blocking layer between the Ag and ZnO, the defect emission was significantly suppressed and the SX emission was enhanced even more as compared to the bare and the Ag NPs directly coated ZnO NRs. The intensities of the phonon replica of DBXs decreased after coating the Ag NPs and Ag NPs/SiO_2 film on the ZnO NRs, which is attributed to the improved surface conditions after applying the coating materials. The enhanced SX emission and reduced phonon replica of DBXs can explain the obvious blue shift of the room temperature PL for the ZnO NRs after coating the Ag NPs and SiO_2 film. A model based on surface states and energy bands theory was proposed to interpret these emission features. The influence of the inserted dielectric layer on the SP–exciton coupling process was

[a]*Wuhan National Laboratory for Optoelectronics, School of Optical and Electronic Information, Huazhong University of Science and Technology, Wuhan, 430074, China. E-mail: zhihao.wu@mail.hust.edu.cn; Fax: +86-27-87793035; Tel: +86-27-87793024*

[b]*Department of Physics/Pen-Tung Sah Institute of Micro-Nano Science and Technology, Xiamen University, Xiamen, 361005, China. E-mail: lijing@xmu.edu.cn; Fax: +86-592-2187196; Tel: +86-592-2181340*

[c]*Department of Photonics and Institute of Electro-Optical Engineering, National Chiao-Tung University, Hsinchu 300, Taiwan*

† Electronic supplementary information (ESI) available. See DOI: 10.1039/c3nr00920c

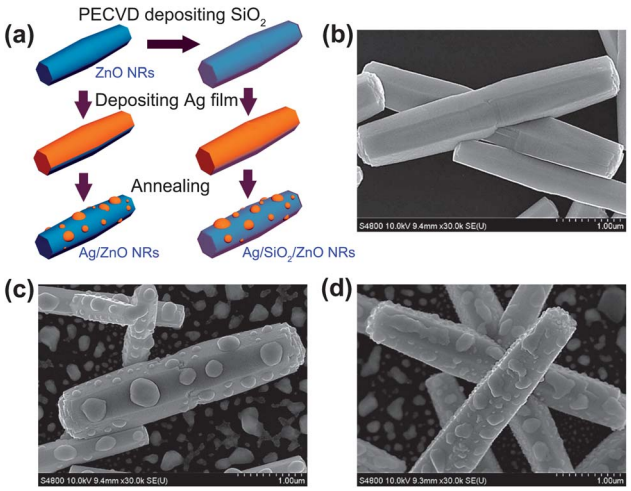

Fig. 1 (a) A schematic illustration of the fabricating process of the samples; (b–d) The SEM images of the as-fabricated samples: bare ZnO NRs, Ag/ZnO NRs and Ag/SiO_2/ZnO NRs, respectively.

also analysed by the TRPL results and the near field distribution on the Ag NP/SiO_2/ZnO nanostructure obtained by FDTD simulation.

Experimental

Dispersed ZnO NRs were grown on seedless substrates (silicon or sapphire) by the hydrothermal method[13] in an acidic solution. The Ag NP/ZnO NR sample was fabricated by depositing a 20 nm thick Ag film on the ZnO NRs, followed by the thermal annealing process, while for the Ag NP/SiO_2/ZnO NR sample an additional SiO_2 layer (10 nm) was deposited on the ZnO NRs by PECVD (Plasma Enhanced Chemical Vapor Deposition) before Ag film deposition, as schematically shown in Fig. 1a. The samples were named as ZnO NRs, Ag/ZnO NRs and Ag/SiO_2/ZnO NRs respectively for simplicity. The morphology and structure properties of the samples were investigated using a Hitachi S-4800 field-emission SEM and TEM (JEM-2100). The crystal structure of the samples was characterized by a Panalytical X'pert PRO XRD with Cu Kα radiation ($\lambda = 1.5406$ Å) in a 2θ range of 20–65°. The evolution of the photoluminescence properties as the surface decoration changes was analysed by TDPL (20–300 K). Temperature-dependent TRPL measurements were carried out to analyze the exciton recombination rate of the samples. The surface plasmon property of the Ag NPs which decorate on the samples was also characterized by the extinction spectra using a UV-visible spectrophotometer Varian Cary 300 (see S1 of the ESI†).

Results and discussion

1 Structure and morphology characterizations

Fig. 1b–d show the SEM images of the bare ZnO NR, Ag/ZnO NR and Ag/SiO_2/ZnO NR samples, respectively. It can be seen that the NRs are dispersively distributed on the substrate with a diameter of ~500 nm and a length of ~4 μm. The Ag NPs

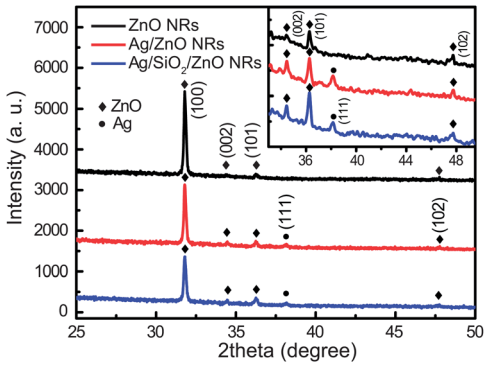

Fig. 2 XRD patterns of the samples: ZnO NRs, Ag/ZnO NRs and Ag/SiO_2/ZnO NRs.

aggregated from the Ag film during the annealing process were randomly attached on the ZnO NRs with diameters ranged from 100 to 300 nm as shown in Fig. 1c. After inserting a thin SiO_2 layer between the Ag and ZnO NRs, the aggregated Ag NPs exhibit some different morphology from that in the Ag/ZnO NRs due to the hydrophilic changes induced by the coated dielectric layer, as shown in Fig. 1d. The XRD patterns of the three samples by a 2 theta–omega scan are shown in Fig. 2. Obviously, the dominant peak at 31.8° (2 theta) should be attributed to the wurtzite ZnO (100) plane diffraction. The strong acidic solution prepared for growth of ZnO NRs forced ZnO NRs to preferentially grow along the wurtzite ⟨0001⟩ direction. Because of the seedless substrates, the synthesized ZnO NRs randomly lied on the silicon substrate with the ⟨0001⟩ direction almost parallel to the substrate surface as shown in Fig. 1. So the ZnO (100) plane diffraction was characterized as the dominant diffraction peak instead of the (002) plane as shown in the XRD patterns. The peak located at 38.1° (2θ) belongs to the Ag (111) plane as manifested in the inset of the figure. The TEM characterization was also carried out as shown in Fig. S2 (ESI†) for all the samples. It can be seen that the results agreed well with the SEM and XRD characterization results. The selected area electron diffraction (SAED) pattern taken from the ZnO NRs indicates the wurtzite crystal structure and the growth direction was along the wurtzite ⟨0001⟩ direction. The thin SiO_2 blocking layer can be clearly seen between the ZnO NRs and coated Ag NPs as shown in Fig. S2c and d,† which demonstrates the formation of an ideal electron blocking layer.

2 Photoluminescence (PL) property

In order to investigate the effects of the decorated Ag metal NPs and the dielectric coating layer on the optical properties of ZnO NRs, room temperature PL (RT-PL) was firstly employed to study the emission properties of these samples. In Fig. 3a, normalized RT-PL spectra of the bare ZnO NR, Ag/ZnO NR and Ag/SiO_2/ZnO NR samples are shown. For the as-grown ZnO NR sample, two peaks of near band edge emission at 3.18 eV and defect emission at 2.75 eV are observed. After coating of the Ag NPs and Ag NP/SiO_2 film, the NBE emission peak has a strong blue shift from 3.18 eV to 3.23 eV. Generally, the NBE emission of ZnO nanostructures at room temperature could shift due to various

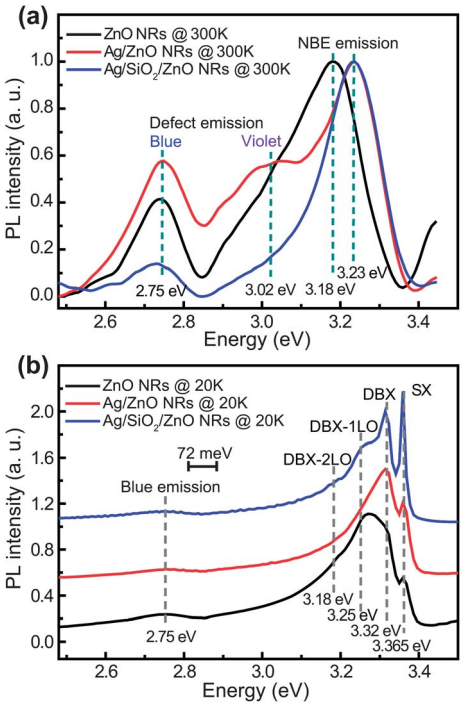

Fig. 3 (a) Room temperature (300 K) PL (RT-PL) spectra of the samples; (b) low temperature (20 K) PL spectra of the samples. The intensity in (a) was normalized to the NBE emission.

reasons, such as laser heating effect, presence of different in-plane stress/strain in the ZnO nanostructure and different contributions of excitonic emissions and their phonon replicas.[14] In our work, all the ZnO NRs were grown under the same conditions and the PL measurements were also performed under the same conditions. Therefore, the contributions of different excitonic emissions from ZnO NRs and their phonon replicas are thought to be responsible for the shift of NBE emission at room temperature.

The defect-related emission also has distinct changes as seen in the RT-PL spectra. The blue emission at about 2.75 eV has been significantly enhanced and another defect-related violet emission at about 3.02 eV also emerges after the direct coating of Ag NPs on the ZnO NRs. This indicates that the direct contact between the Ag and ZnO NRs promotes the defect emission rather than suppressing it, which is undesirable for applications. In contrast, the defect-related emission has been drastically suppressed after introducing the SiO_2 thin film layer between the Ag NPs and ZnO NRs. The luminescence properties of ZnO nanostructures have been improved after coating with dielectric[10] or polymer materials,[11,12] which can passivate the surface defects and decrease the polarization effect, and thus lead to the redistribution of excitons in ZnO. Noble metal nanoparticles have been widely used for enhancing the spontaneous recombination rate in semiconductor materials due to the coupling effect between local surface plasmons (SPs) and excitons.[2,15] Therefore, it is proposed that the evolution of the RT-PL spectra of the samples should come from the localized surface plasmon resonance (LSPR) effect of Ag NPs and the surface condition modification after coating the Ag NPs and Ag NP/SiO_2 film.

In order to further reveal the variation in luminescence properties of ZnO NRs when coated with the Ag NPs and Ag NP/SiO_2 film, the temperature-dependent (20–300 K) NBE emission spectra of all the samples were collected. At low temperature (20 K, shown in Fig. 3b), all the samples exhibit three main emission peaks located near the band edge and a defect-related emission peak located in the blue region. The emission peak located at 3.365 eV (368.0 nm) is frequently observed for ZnO NWs or NRs and is correlated with the surface exciton (SX) recombination characteristic of the large specific surface area in the nanostructure.[16] Another main recombination emission peak at 3.32 eV (373.5 nm) should be attributed to the defect bound exciton (DBX) and is usually named as A-line.[17] Considering the longitudinal-optical (LO) phonon energy of ZnO (72 meV), the other two emission peaks that can be resolved in the lower energy side of near band edge should be unambiguously assigned to the first and the second order LO phonon replica of the DBX-line: DBX-1LO (3.25 eV) and DBX-2LO (3.18 eV), respectively. The broad blue emission at 2.75 eV (451.0 nm) is related to the intrinsic defect of Zn interstitials as reported in the literature.[18] For the as-grown sample, the first order LO phonon replica of the DBX is the dominant emission and only weak SX emission can be resolved in the higher energy regime. It is found that after the coating of Ag NPs, the SX intensity increases evidently, and the DBX peak becomes strongest. For the Ag/SiO_2/ZnO NR sample, the SX emission has been further enhanced to be the strongest one. The phonon replicas of the DBX peaks are suppressed for both the Ag/ZnO NR and Ag/SiO_2/ZnO NR samples.

The temperature-dependent (20–300 K) NBE emission spectra of all the samples are shown in Fig. 4a–c. As the temperature increases gradually, the intensities of SX and DBX emissions become weaker and the peak shifts towards lower energy for the three samples. However, the dominant emission lines display different behaviours for the ZnO NRs coated with the Ag NPs and Ag NP/SiO_2 film compared with those in the bare ZnO NRs as the temperature increases. For the as-grown ZnO NR sample, the first order phonon replica of the DBX dominates the emission spectra at low temperature and still keeps as the strongest peak at room temperature. While for both the ZnO NR samples coated with Ag NP and Ag NP/SiO_2 films, the DBX emission line dominates the spectra instead of its phonon replica as the temperature rises to 300 K. Clearly, the variation in excitonic emissions and their phonon replicas result in the observed strong blue shift of the NBE emission at room temperature (shown in Fig. 3a) for the Ag/ZnO NR and Ag NP/SiO_2/ZnO NR samples in comparison with the as-grown ZnO NRs. Note that the intensity of the SX emission line decreases slowly with increasing temperature for both the Ag/ZnO NR and Ag/SiO_2/ZnO NR samples and it can be still clearly seen as a shoulder at room temperature, as shown in Fig. 4b and c. It can also be noticed that an additional violet defect-related emission gradually appears as the temperature rises for the Ag/ZnO NR sample, which can be seen clearly in the room temperature PL spectra in Fig. 3a.

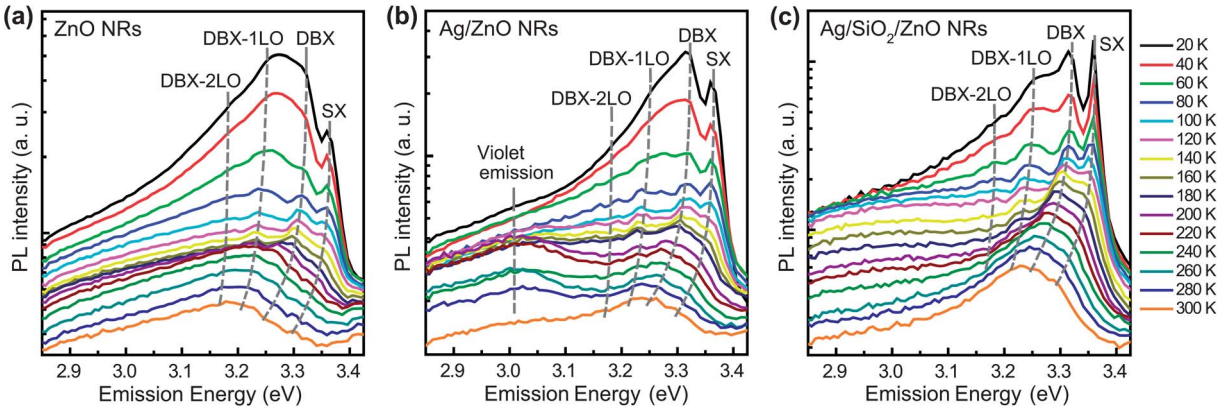

Fig. 4 Temperature-dependent PL (TDPL) spectra obtained from (a) ZnO NR, (b) Ag/ZnO NR and (c) Ag/SiO_2/ZnO NR samples.

As a polar semiconductor, ZnO experiences a strong Fröhlich interaction (FI) that results in the exciton–phonon interaction. The interaction is relatively small in a perfect crystal due to parity conservation, and would be highly enhanced in ZnO nanostructures for their large surface-to-volume ratio and abundant surface defects.[14,19,20] It is evident that the phonon–exciton coupling effect can be suppressed by passivating the surface defects of ZnO nanostructures.[19,20] In our work, the surface states of ZnO NRs have been effectively passivated by coating materials, such as the Ag NPs and SiO_2 film, which leads to weaker phonon-assisted exciton emission and thus results in the apparent blue shift of NBE emission for the Ag/ZnO NR and Ag NP/SiO_2/ZnO NR samples at room temperature. Since the SX emission mainly arises from the excitons trapped at the surface region, the improved SX emission after coating of Ag NP and Ag NP/SiO_2 films indicates that the band structure near the surface area of ZnO NRs has been altered to different states which increase the radiative recombination probability for the surface excitons. The variation of defect-related emission in different samples should also be associated with redistribution of carriers and modification of exciton recombination rates in the ZnO.

In order to understand the variations of SX and the defect-related emissions from different ZnO NR samples, a model based on different types of contacts formed between metals, ZnO and SiO_2 blocking layer is proposed to interpret these changes. Fig. 5 shows the energy band alignment diagrams of bare ZnO NRs, Ag/ZnO NRs and Ag NPs/SiO_2/ZnO NRs. For the as-grown ZnO NR sample, free electrons is the majority carriers since unintentionally doped ZnO exhibits n-type conductivity due to its intrinsic defects, such as oxygen vacancies.[21] The surface defects and the adsorption of O_2 or H_2O molecules at the surface of ZnO NRs will trap negatively charged free electrons, and result in a positively charged depletion region, which generates upward band-bending near the surface. The photo-generated electron–hole pairs in the depletion region will be spatially separated due to the potential variation near the surface, as illustrated in Fig. 5a. The separated carriers would radiatively recombine in two ways: one is the direct recombination which contributes to the SX emission, and another one is that the excess holes at the surface tunnel into the deep level centers inside the NRs and produce defect-related emission. The SX emission is relatively weak due to the small electron–hole wave function overlap, making the DBX emission from the bulk region of ZnO NRs dominate the luminescence spectra. When the ZnO NRs are directly coated with Ag NPs, since the work function for Ag (4.26 eV) is lower than that for ZnO (5.2 eV and its first electron affinity is about 4.3 eV), electrons will migrate from Ag to the conduction band of ZnO to achieve the

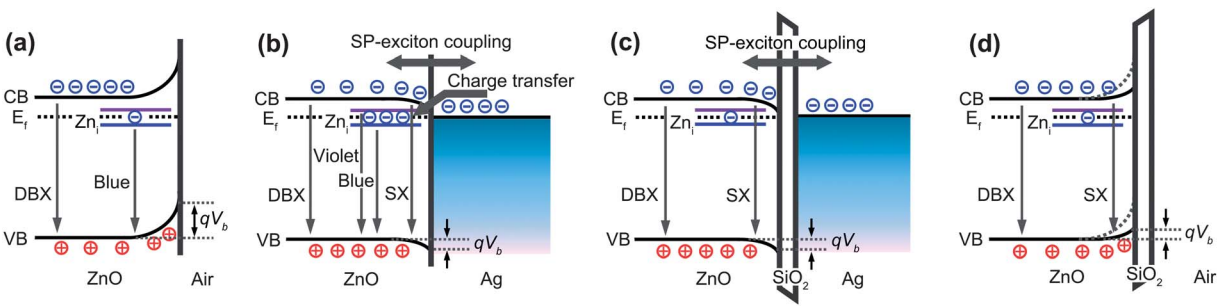

Fig. 5 Band alignment diagrams of bare ZnO NRs and those in contact with different materials: (a) upward band bending for the bare ZnO NRs exposed in air due to the depletion of surface donor states. A relatively high built-in-barrier (qV_b) is formed. (b) The effective band bending has been reduced within this as-formed Ohmic contact interface between Ag NPs and ZnO NRs. The qV_b is also reduced and the SX emission is increased due to the improved overlap of the wave functions of electrons and holes at the surface region. Defect-related emission is enhanced due to the charge transfer process. (c) The band bending is also decreased after introducing a thin SiO_2 blocking layer. The SX emission is increased and the charge transfer process is suppressed. (d) As-formed type I heterostructures between ZnO/SiO_2 and the band bending is decreased.

Fermi level equilibrations, forming Ohmic type of Ag/ZnO contact.[22] The Ohmic contact between the ZnO nanowire and Ag has also been demonstrated experimentally in the literature.[23,24] A schematic of the energy band alignment for the interface of Ag NPs/ZnO NRs is shown in Fig. 5b. Electrons are accumulated near the ZnO surface, leading to downward band bending. However, the potential variation (qV_b) is much lower than the as-grown ZnO NRs because of the small difference between the electron affinity of ZnO and the work function of Ag. In addition, the width for the accumulation region is much smaller than that for the depletion regions at the surface of the as-grown ZnO due to the much higher density of accumulated electrons than the depleted donor. The lower qV_b as well as the narrower band-bending region will lead to a higher electron–hole wave function overlap, which results in an increased SX emission as displayed in the temperature-dependent PL spectra in Fig. 4b. On the other hand, as the energy level for the donor-like defects such as Zn interstitial is close to the Fermi level, when excited the direct contact between the metal and semiconductor will facilitate the transfer of electrons from the metal NPs to the defects in ZnO, enhancing the defect-related emission. Therefore, the additional violet emission and the enhanced blue emission as shown in Fig. 3a and 4b for the Ag/ZnO NR sample should come from the expanded Zn interstitial defect,[18] which is attributed to the charge transfer process from the metal to the defect centers.

A thin SiO_2 layer can eliminate the charge transfer process through the as-formed type-I band-energy alignment of the SiO_2/ZnO interface with a conduction band offset of 4.7 eV and a valence band offset of 0.9 eV.[25] Fig. 5c schematically shows the energy band alignment of Ag/SiO_2/ZnO heterojunctions. The 10 nm thick SiO_2 blocking layer is sufficiently thick to effectively prevent the electrons in the Ag side from transferring to the defect level of ZnO, and it is thin enough to retain effective SP–exciton coupling between Ag and surface excitons in ZnO, which reduces defect emission and enhances SX emission. In addition, the SiO_2 coating layer can also act as a dielectric layer as reported in the literature[10,12] to passivate the surface states and thus reduce the potential variation and narrow the depletion region near the ZnO surface, which in turn can improve the overlap of the wave functions of electrons and holes, as shown in Fig. 5d. So we can conclude that the significantly enhanced SX emission and reduced defect-related emission for the Ag/SiO_2/ZnO NR sample are attributed to the improved surface condition of ZnO NRs owing to the direct coating of the SiO_2 dielectric layer.

3 TRPL characterization

Although inserting a SiO_2 blocking layer between Ag NPs and ZnO NRs can effectively suppress the defect-related emission by eliminating the charge transfer process, the SP-coupling effect may be inevitably weakened because of the increased coupling distance after introducing the SiO_2 blocking layer. In order to determine the coupling effect as well as the exciton recombination rate after coating the Ag NPs and Ag NPs/SiO_2 layer on the ZnO NRs, measurements of

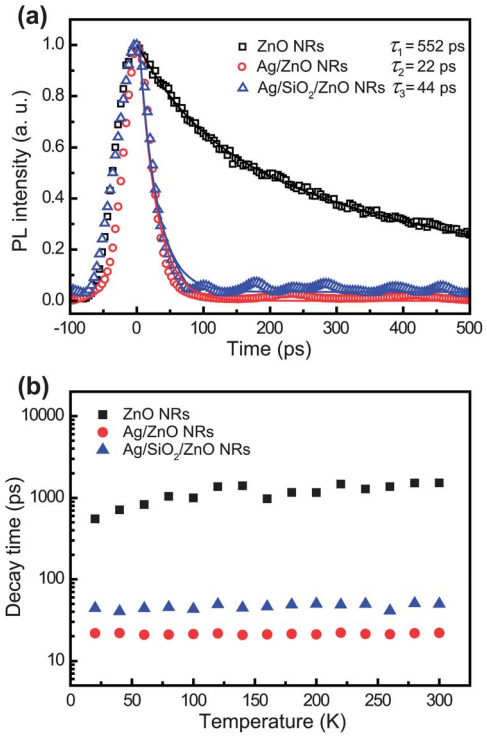

Fig. 6 (a) Low temperature (20 K) TRPL spectra of bare ZnO NR, Ag/ZnO NR and Ag/SiO_2/ZnO NR samples. (b) The decay time as a function of temperature for the samples.

temperature-dependent TRPL at the band edge of ZnO were carried out. A picosecond pulsed laser was sent to the sample and the luminous intensity from the samples was recorded by a time-resolved system after the pulsed laser was closed. The luminous intensity decay curve generally performances as an exponential decay curve and the measured effective PL lifetime (τ_{PL}) is the time when the intensity drops to $1/e$. At 20 K as shown in Fig. 6a, the effective PL lifetimes are measured to be 552, 22 and 44 ps, respectively. It is obvious that the recombination rate for excitons near the band edge in ZnO has been greatly improved after decorating with the Ag NPs due to the SP–exciton coupling.[2,15,26] As compared to the Ag NP/ZnO NR sample, the recombination rate of the Ag NP/SiO_2/ZnO NR sample is expectantly lower due to the increased coupling distance. However, the recombination rate is still more than 10 times larger than the bare ZnO NRs, which indicates that the SP–exciton coupling effect is still strong even with the thin SiO_2 layer. Similar results have also been reported that after introducing a dielectric layer between the metal nanostructure and ZnO, the luminescence of the ZnO NRs can still be enhanced.[27] The temperature dependence of decay time for ZnO NBE emission in those three samples is shown in Fig. 6b. It can be found that the decay time of excitons in ZnO NRs exhibits some increasing trend as the temperature rises from 20 to 300 K. In spite of the fact that the delocalization of excitons by the thermal energy would enhance the exciton recombination rate, the nonradiative recombination processes are also activated as the temperature rises, which result in an extended lifetime of NBE excitons, which can be

evidenced by the bi-exponential fitting results (not shown here). Compared with the bare ZnO NR sample, both the recombination rates in the Ag/ZnO NR and Ag/SiO_2/ZnO NR samples are obviously enhanced in the entire temperature range and are almost independent of temperature changes. Thus, the SP–exciton coupling process dominates the recombination process.

4 FDTD simulation

To gain insight into the origin of this SP–exciton coupling between the Ag NPs and ZnO NRs, further FDTD calculations were carried out to analyse the local enhanced *E*-field originated from the LSPR effect of the Ag NPs on the samples. Fig. 7 shows the simulated near-field distribution for a typical Ag NP (diameter of 150 nm) directly located on the surface of a bare ZnO NR and in the case of an Ag NP isolated by a thin SiO_2 film. The incident light wavelength was 375 nm (3.31 eV) which located at the band edge of ZnO. It can be found that a strong local enhanced *E*-field can be obtained near the Ag NP. The obtained *E*-field pattern with a similar four-lobe field distribution for the Ag NP demonstrates a high order LSP resonance mode[28] as that has been reported in our previous work.[29] In Fig. 7b, it can be noticed that the *E*-field intensity near the surface of ZnO seems not as strong as that in Fig. 7a due to the isolation of the Ag NP away from the ZnO surface by the SiO_2 film. However, a highly local confined *E*-field can be obtained within the SiO_2 layer for the Ag NP/SiO_2/ZnO nanostructure as shown in Fig. 7b. The substrate or dielectric layer has been demonstrated to have an important role in the SPR properties of the metal nanostructures.[30] The nanoscale metal-oxide–semiconductor (MOS) hybrid plasmonic structure has the ability to confine the electromagnetic field in the low dielectric-constant oxide nanogap, which greatly reduces the plasmonic loss and enables the application in plasmonic nanolaser.[31,32] Therefore, in this work, the efficient coupling between the SP and exciton in ZnO can still be realized across the gap formed by the thin SiO_2 dielectric layer through the highly confined *E*-field. Additionally, a comparably strong local field distribution in ZnO can be achieved due to the LSPR effect of Ag NPs even there is an insertion of a thin SiO_2 dielectric layer between them.

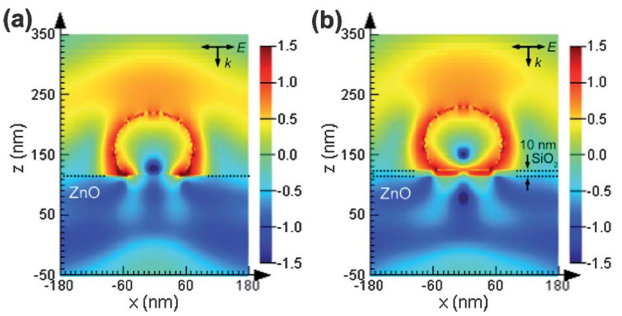

Fig. 7 Near-field distribution under 3.31 eV (375 nm) light illumination for a typical Ag NP (diameter of 150 nm) located on the surface of (a) ZnO NRs and (b) SiO_2 film/ZnO NRs obtained by FDTD simulation. The incident direction and the polarization are shown in the figure.

Conclusions

In conclusion, the effects of metal NPs on the optical properties of ZnO NRs have been systematically investigated using the temperature-dependent PL and time-resolved PL characterizations. As compared to the case of bare ZnO NRs, it is found that remarkable enhancement in surface exciton emission and reduction in phonon-assisted exciton emission for the ZnO NRs can be achieved by direct coating of the Ag NPs. However, the direct contact of Ag NPs/ZnO NRs leads to notable increment of blue and violet emission from the Zn interstitial defects due to the charge transfer process, which is not favourable in terms of improving luminescence properties of ZnO. The disadvantages of this metal–semiconductor direct contact can be effectively suppressed by coating a thin dielectric layer, such as SiO_2, between Ag NPs and ZnO NRs while keeping the surface-plasmon–exciton coupling effect strong, which is of great importance to improve the emission properties of nanostructured semiconductors. The variation of the optical properties of ZnO NRs with different surface coating schemes has been explained using a model based on the different contacts formed between metals, ZnO and blocking layer. This work provides an inside study on the practical application of SPR effects from metal NPs for luminescence improvement in wide band gap (WBG) materials, such as ZnO or GaN, and related optoelectronic devices.

Acknowledgements

This work was supported by the National Basic Research Program of China (Grant no. 2012CB619302, 2010CB923204 and 2009CB930704), National Natural Science Foundation of China (61106118), Natural Science Foundation of Fujian Province of China (2011J01362), and Fundamental Research Funds for the Central Universities (2011121026).

Notes and references

1 L. Zhao, T. Ming, H. J. Chen, Y. Liang and J. F. Wang, *Nanoscale*, 2011, **9**, 3849.
2 K. Okamoto, I. Niki, A. Shvartser, Y. Narukawa, T. Mukai and A. Scherer, *Nat. Mater.*, 2004, **3**, 601.
3 D. M. Yeh, C. F. Huang, C. Y. Chen, Y. C. Lu and C. C. Yang, *Appl. Phys. Lett.*, 2007, **91**, 171103.
4 Q. Qiao, C. X. Shan, J. Zheng, B. H. Li, Z. Z. Zhang, L. G. Zhang and D. Z. Shen, *J. Mater. Chem.*, 2012, **22**, 9481.
5 H. Shen, C. X. Shan, Q. Qiao, J. S. Liu, B. H. Li and D. Z. Shen, *J. Mater. Chem. C*, 2013, **1**, 234.
6 Ü. Özgür, Y. I. Alivov, C. Liu, A. Teke, M. A. Reshchikov, S. Doğan, V. Avrutin, S. J. Cho and H. Morkoç, *J. Appl. Phys.*, 2005, **98**, 041301.
7 Z. L. Wang, *Mater. Today*, 2004, **7**, 26.
8 C. Klingshirn, R. Hauschild, H. Priller, M. Decker, J. Keller and H. Kalt, *Superlattices Microstruct.*, 2005, **38**, 209.
9 C. Klingshirn, H. Priller, M. Decker, J. Brückner, H. Kalt, R. Hauschild, J. Zeller, A. Waag, A. Bakin, H. Wehmann, K. Thonke, R. Sauer, R. Kling, F. Reuss and Ch. Kirchner, *Adv. Solid State Phys.*, 2005, **45**, 261.

10 J. P. Richters, T. Voss, D. SKim, R. Scholz and M. Zacharias, *Nanotechnology*, 2008, **19**, 305202.
11 J. P. Richters, T. Voss, L. Wischmeier, I. Rückmann and J. Gutowski, *Appl. Phys. Lett.*, 2008, **92**, 011103.
12 K. W. Liu, R. Chen, G. Z. Xing, T. Wu and H. D. Sun, *Appl. Phys. Lett.*, 2010, **96**, 023111.
13 L. Vayssieres, *Adv. Mater.*, 2003, **15**, 464.
14 C. H. Ahn, S. K. Mohanta, N. E. Lee and H. K. Cho, *Appl. Phys. Lett.*, 2009, **94**, 261904.
15 A. Neogi, C. W. Lee, H. O. Everitt, T. Kuroda, A. Tackeuchi and E. Yablonovitch, *Phys. Rev. B: Condens. Matter Mater. Phys.*, 2002, **66**, 153305.
16 L. Wischmeier, T. Voss, I. Ruckmann, J. Gutowski, A. C. Mofor, A. Bakin and A. Waag, *Phys. Rev. B: Condens. Matter Mater. Phys.*, 2006, **74**, 195333.
17 C. Bekeny, T. Voss, B. Hilker, J. Gutowski, R. Hauschild, H. Kalt, B. Postels, A. Bakin and A. Waag, *J. Appl. Phys.*, 2007, **102**, 044908.
18 H. B. Zeng, G. T. Duan, Y. Li, S. K. Yang, X. X. Xu and W. P. Cai, *Adv. Funct. Mater.*, 2010, **20**, 561.
19 W. K. Hong, G. Jo, M. Choe, T. Lee, J. I. Sohn and M. E. Welland, *Appl. Phys. Lett.*, 2009, **94**, 043103.
20 R. Chen, Q. L. Ye, T. C. He, T. Wu and H. D. Sun, *Appl. Phys. Lett.*, 2011, **98**, 241916.
21 S. B. Zhang, S. H. Wei and A. Zunger, *Phys. Rev. B: Condens. Matter Mater. Phys.*, 2001, **63**, 075205.
22 J. Yin, Y. S. Zang, C. Yue, Z. M. Wu, S. T. Wu, J. Li and Z. H. Wu, *J. Mater. Chem.*, 2012, **22**, 7902.
23 Z. L. Wang and J. H. Song, *Science*, 2006, **312**, 242.
24 J. H. Song, J. Zhou and Z. L. Wang, *Nano Lett.*, 2006, **6**, 1656.
25 J. B. You, X. W. Zhang, H. P. Song, J. Ying, Y. Guo, A. L. Yang, Z. G. Yin, N. F. Chen and Q. S. Zhu, *J. Appl. Phys.*, 2009, **106**, 043709.
26 I. Gontijo, M. Boroditsky, E. Yablonovitch, S. Keller, U. K. Mishra and S. P. DenBaars, *Phys. Rev. B: Condens. Matter Mater. Phys.*, 1999, **60**, 11564.
27 Q. Qiao, C. X. Shan, J. Zheng, H. Zhu, S. F. Yu, B. H. Li, Y. Jia and D. Z. Shen, *Nanoscale*, 2013, **5**, 513.
28 K. L. Kelly, E. Coronado, L. L. Zhao and G. C. Schatz, *J. Phys. Chem. B*, 2003, **107**, 668.
29 Y. S. Zang, X. He, J. Li, J. Yin, K. Y. Li, C. Yue, Z. M. Wu, S. T. Wu and J. Y. Kang, *Nanoscale*, 2013, **5**, 574.
30 H. J. Chen, T. Ming, S. R. Zhang, Z. Jin, B. C. Yang and J. F. Wang, *ACS Nano*, 2011, **5**, 4865.
31 R. F. Oulton, V. J. Sorger, D. A. Genov, D. F. P. Pile and X. Zhang, *Nat. Photonics*, 2008, **2**, 496.
32 R. F. Oulton, V. J. Sorger, T. Zentgraf, R. M. Ma, C. Gladden, L. Dai, G. Bartal and X. Zhang, *Nature*, 2009, **461**, 629.

